VIP Magnetic Materials

DOI: 10.1002/ange.201205843

A Genuine Two-Dimensional Ising Ferromagnet with Magnetically Driven Re-entrant Transition**

*Houria Kabbour, Rénald David, Alain Pautrat, Hyun-Joo Koo, Myung-Hwan Whangbo, Gilles André, and Olivier Mentré**

Inorganic compounds made up of low-dimensional ferromagnetic (FM) units display fascinating properties and provide a rich opportunity to investigate FM ground states, field-induced transitions,[1] and magnetization steps.[2–4] Even the spin-valve effect, realized in multilayer thin films, is found in the magnetic metal $Ca_3Ru_2O_7$[5] and its Cr-doped analogue[6] in which FM double-perovskite layers are antiferromagnetically coupled.[7] The inorganic compound $Cr_2Si_2Te_6$, also consisting of FM layers,[8a,b] turns out to be a unique example of a bulk 2D FM Ising system.[8c]

It is a great synthetic challenge to discover new magnetic transition-metal oxides made up of FM layers. In searching for such materials, a rational approach rather than by a blind exploration of chemical systems should be used. In general, a transition-metal cation at a coordinate site with three-fold or higher rotational symmetry can lead to uniaxial magnetism if its d electron count and spin state are such that there occurs an unevenly-filled degenerate level, as found for high-spin Fe^{2+} ions at linear-coordinate sites[8a] and high-spin Co^{3+} and Co^{2+} ions at trigonal-prismatic sites.[8b,c] In principle, high-spin $Fe^{2+}O_6$ octahedra can support uniaxial magnetism as long as they possess three-fold rotational symmetry. It can be imagined that isolated FM layers form from such FeO_6 octahedra by edge-sharing because the Fe-O-Fe angle will be close to 90° so that the nearest-neighbor spin exchange would be FM.

Our guided search for such a magnetic system led to the synthesis of $BaFe_2(PO_4)_2$ that turns out to be the first oxide 2D Ising ferromagnet. It consists of FM honeycomb layers of edge-sharing FeO_6 octahedra containing high-spin Fe^{2+} ions. Such FeO_6 octahedra showing uniaxial magnetism are expected to be susceptible to Jahn–Teller (JT) instability.[9] Indeed, on cooling, $BaFe_2(PO_4)_2$ undergoes a rare re-entrant structural transition owing to the competition between uniaxial magnetism and the JT distortion.

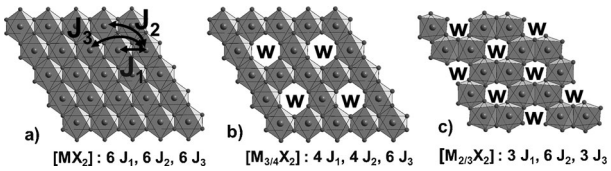

Figure 1. Comparison of a) triangular, b) Kagomé, and c) honeycomb lattices geometries (W = windows).

The three main 2D triangular lattices consisting of edge-sharing MO_6 octahedra are shown in Figure 1. Starting from the $[MO_2]$ triangular lattice, the ordering of one quarter of the M vacancies leads to the $[M_{3/4}O_2]$ Kagomé lattice, and that of one third of the M vacancies to the $[M_{2/3}O_2]$ honeycomb lattice. They all possess similar intralayer spin exchange paths in different ratios (Figure 1). The superexchange (SE) path J_1 consists of two M-O-M bridges with a M-O-M angle of about 90°, while the super-superexchange (SSE) paths J_2 and J_3 involve M–O···O–M bridges. For M = Fe, it is expected that the 90° SE J_1 path is ferromagnetic (FM) for high-spin (HS) Fe^{2+} (d^6, $S = 2$) but antiferromagnetic (AFM) for HS Fe^{3+} (d^5, $S = 5/2$) cations, according to dominant direct t_{2g}–t_{2g} overlaps.[10] Results of a literature search for such magnetic iron oxides with pertinent 2D or pseudo 2D lattices are summarized in Table 1,[11–13] which indicates that the Fe^{2+} ions is the key cation leading to significant intralayer magnetic moment, and that only a few pertinent crystal structures are known. We note that truly decoupled magnetic units require a much

Table 1: Characteristics of different layered compounds with spatially disconnected triangular-related Fe lattices.

M	Triangular	Kagomé	Honeycomb
Fe^{2+}	LDH-$Fe(OH)_2$ in-plane FM, inter-plane AFM $T_N = 34$ K, $d_\perp = 4.5$ Å	No	$BaFe_2(PO_4)_2$ This work 2D-Ising FM
Fe^{3+}	Delafossite $Ag^+Fe^{3+}O_2$ in-plane AFM $T_N = 16$ K, $d_\perp = 6.2$ Å	normal spinel $Zn^{2+}Fe^{3+}{}_2O_4$ in-plane AFM $T_N = 10$ K, $d_\perp = 4.9$ Å	No

[*] Dr. H. Kabbour, R. David, Dr. O. Mentré
Univ. Lille Nord de France, CNRS UMR8181, Unité de Catalyse et de Chimie du Solide, UCCS USTL
F-59655 Villeneuve d'Ascq (France)
E-mail: olivier.mentre@ensc-lille.fr
Dr. A. Pautrat
CRISMAT, UMR 6508-CNRS, ENSICAEN (France)
Dr. H.-J. Koo
Dpt of Chemistry and Research Institute of Basic Science, Kyung Hee University (Korea)
Prof. M.-H. Whangbo
Dpt of Chemistry, North Carolina State University (USA)
Dr. G. André
LLB, CEA-Saclay, bât. 563-91191 Gif-sur-Yvette (France)

[**] This work was carried out under the framework of the MAD-BLAST project supported by the ANR (Grant ANR-09-BLAN-0187-01).

Supporting information for this article is available on the WWW under http://dx.doi.org/10.1002/anie.201205843.

© 2012 Wiley-VCH Verlag GmbH & Co. KGaA, Weinheim

greater spatial separation between the magnetic layers than found in the examples presented.

$BaCo_2(AsO_4)_2$ and its analogues are built from a 2D honeycomb array.[14] The magnetic decoupling between such units result from the circa 8 Å spacing between them. Below $T_N = 5.3$ K, it exhibits stepwise magnetization and a complex magnetic ground state based on a helicoidal spin arrangement with 2D XY magnetic character.[15] In this $BaM_2X_2O_8$ (M = Ni, Co; X = P, V, As) family, $BaCo_2As_2O_8$ and $BaNi_2P_2O_8$ ($T_N = 23.5$ K)[15b] are 2D XY antiferromagnets, while $BaNi_2V_2O_8$ ($T_N = 50$ K) has been proposed to be a 2D weakly anisotropic Heisenberg antiferromagnet.[16] Predominant intralayer AFM interactions with d^7 or d^8 ions may be due to weakly FM J_1. The incorporation of HS Fe^{2+} ions in this lattice is expected to strengthen FM J_1 due to the direct FM t_{2g}–t_{2g} exchanges.[10] However, no Fe^{2+} analogue of this family has been reported so far. Furthermore, contrary to the Co^{2+} analogues favoring a XY character, a large number of Fe^{2+} compounds including layered systems exhibit an Ising character,[17] which is ideal for achieving uniaxial magnetism.

The synthesis of the hypothetical phases $BaFe_2(XO_4)_2$ (X = P, V, As) could not be achieved by solid-state routes under various conditions designed to stabilize Fe^{2+} cations. Therefore, we attempted hydrothermal synthesis, used for $BaCo_2(AsO_4)_2$,[18] adding hydrazine (H_2N-NH_2) to stabilize Fe^{2+} ions in the feeding solution. For X = As, unexpected phases were formed, leading to the reduced species As^{3+}. For X = P, however, high-quality single crystals of $BaFe_2(PO_4)_2$ were grown (Supporting Information, S0). The synthesis of high-yield $BaFe_2(PO_4)_2$ for powder neutron diffraction (PND) was achieved using microwave assisted-treatment (see the Experimental Section and Supporting Information, S1). $BaFe_2(PO_4)_2$ is isomorphous with other compounds of the series, with a interlayer separation of 7.8 Å ($c/3$), a = 4.8730(2), $c = 23.368(2)$, space group $R\bar{3}$, $R_F = 4.03\,\%$, and $wR_{F2} = 4.99\,\%$. The FeO_6 octahedra are regular (Fe–O: three of 2.114(5) Å, three of 2.140(5) Å) share all corners with PO_4 tetrahedra pointing towards the interlayer spacing (Figure 2).

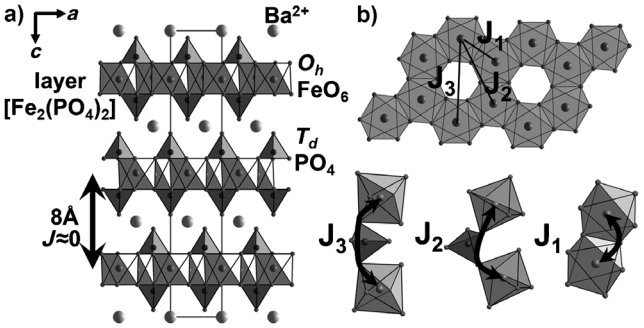

Figure 2. a) Crystal structure of $BaFe_2(PO_4)_2$. b) Projection of the $Fe_2(PO_4)_2$ layer in the *ab* plane.

The Fe-O-Fe angle of the J_1 path is 83°, while J_2 and J_3 have O···O contacts that are shorter than the sum of the Van der Waals radii (Supporting Information, S1).

To determine magnetic properties, 5 mg of the crystals were isolated, crushed, and blocked into cellophane. $\chi(T)$

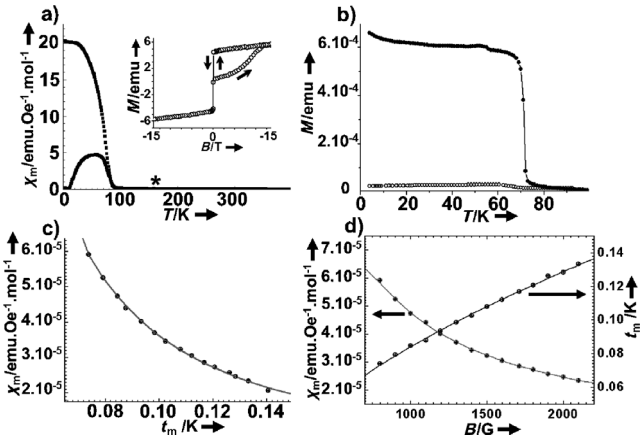

Figure 3. a) $\chi_m(T)$ (FC/ZFC at B = 100 G). Inset: M(H) at $T = 4$ K (coercivity $B_c < 50$ G). * indicates the structural transition at about 150 K. b) Magnetization at 1000 G on aligned single crystals. ○ in-plane, ● out-of-plane. c), d) Scaling plots and extraction of the critical exponents ($\gamma = 1.73$, $\delta = 17$, $\beta = 0.12$) of the FM transition. c) $\chi_m \propto t_m^{-\gamma}$, $\gamma = 1.73(8)$; d) $\chi_m B^{1/(\delta-1)}$, $\gamma = 17(3)$; $t_m \propto B^{1/(\gamma+\beta)}$, $\gamma+\beta = 1.85(7)$. χ_m is the temperature- and field-dependent maximum of the magnetic susceptibility.

shows a sharp FM transition towards a long-range order around 80 K and a divergence between the zero-field-cooled (ZFC) and field-cooled (FC) curves, with a broad maximum at about 70 K (Figure 3a). Our ac susceptibility measurements after fitting of scaling equations (see below) gives T_c = 65.5 K. At about 150 K, a weak anomaly occurs from a lattice distortion (discussed below). Above 200 K, the fitted Curie–Weiss law (Supporting Information, S2a) yields $\mu_{eff} = 6.16\ \mu_B$/Fe and $\theta_{cw} = 56.5$ K, which shows a pronounced orbital contribution (spin-only $\mu_{eff} = 4.9\ \mu_B/Fe^{2+}$). At 4 K, the first magnetization branch shows irreversible effects (grain reorientation and/or domain walls motion), while upon further field variation, the $M(H)$ curve shows an abrupt reversible reversal of the spins with a strong remanent moment (M_{rem} = 4.2 μ_B per formula unit (FU)), together with a weak coercitivity of 50 Oe (Figure 3a, inset). Fields of up to 14 Tesla led to the maximal moment M = 6 μ_B/FU, which is lower than $M_s = 8\ \mu_B$ expected for two Fe^{2+} ($S = 2$) cations. Approximating the uniaxial behavior of the grains toward the magnetic field by the relation $M_{rem}/M_s = 0.5$[19] leads to $M_s = 8\ \mu_B$, so the magnetic saturation should be sought at stronger fields. Magnetic measurements performed on oriented stack of six small single crystals show a strongly anisotropic character, with a magnetic easy axis parallel (∥) to the c axis ($M_\parallel \approx 20\,M_\perp$), (Figure 3b). The $M(H)$ square curve is reminiscent of 2D FM domains weakly coupled by interlayer exchanges, as already observed for the 2D Heisenberg FM Cs_2AgF_4 with $S = 1/2$ Ag^{2+} ions.[20,21]

A 2D Ising ferromagnet is a well-known exception for the Mermin–Wagner theorem, which excludes broken (magnetic) symmetries in 2D systems but favors magnetic fluctuations rather than long-range ordering (LRO).[22] The ac susceptibility of $BaFe_2(PO_4)_2$ measured at about T_c (60 to 70 K) in nonzero static biasing applied fields ($0\ T < H_a < 0.3$ T) reveals a series of peaks/critical maxima at temperature T_m. Under

© 2012 Wiley-VCH Verlag GmbH & Co. KGaA, Weinheim

increasing/decreasing H_a, the susceptibility data are fully reversible and show no sample reorientation (Supporting Information). The critical maxima are generally understood in terms of the fluctuation–dissipation theorem.[23] According to the conventional static scaling law,[24] their variation with field and temperature are governed by a series of power laws driven by critical exponents. Using a previously reported procedure and expressions,[25] we extracted the critical exponents $\gamma = 1.73(8)$, $\beta = 0.12(7)$, and $\delta = 17(3)$ (see Figure 3c,d) in excellent agreement with the 2D Ising critical parameters ($\gamma = 1.75$, $\beta = 0.125$, $\delta = 15$). Thus, together with the easy magnetization parallel to c, we conclude that $BaFe_2(PO_4)_2$ is a unique example of a 2D Ising ferromagnet transition-metal oxide. To our knowledge, $Cr_2Si_2Te_6$[8] is the only inorganic compound with 2D FM Ising compound ($\beta =$ 0.17 from neutron scattering experiment).

To investigate the re-entrant transition and magnetic structure, $BaFe_2(PO_4)_2$ was studied by PND at the Laboratoire Leon Brillouin using the G41 diffractometer ($\lambda =$ 2.4226 Å) from 288 K to 1.8 K. We note several phenomena upon cooling (see Figure 4a):

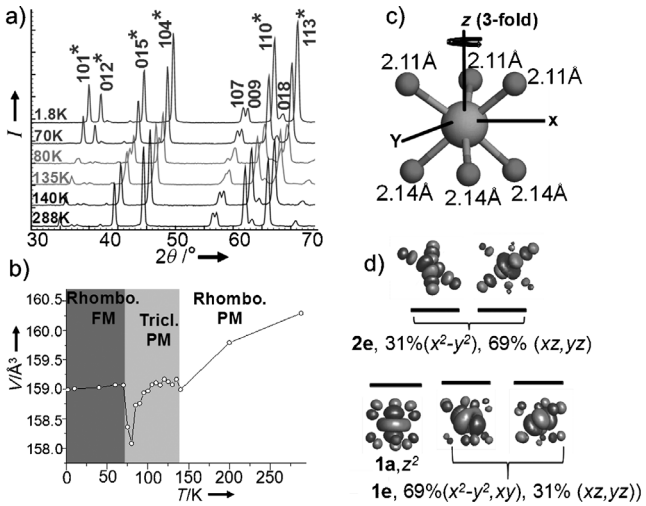

Figure 4. a) Evidence of the re-entrant transition on ND patterns. * show FM contributions below T_c. b) Magnetic phase diagram (PM for paramagnetic, FM for ferromagnetic) along with the volume of the asymmetric cell. c) Geometry of the FeO_6 octahedra at 300 K. d) Crystal-field degenerate levels.

- From room temperature to 140 K, the rhombohedral symmetry is preserved and the standard thermal lattice contraction is observed;
- From 135 K to 75 K, a sensitive splitting of the diffraction peaks occurs, which has a maximum at 80 K. This corresponds to the $\chi(T)$ anomaly detected at 150 K. The unit cell corresponds to a primitive triclinic lattice with a volume one third of those of the rhombohedral lattice. Note that the $P\bar{1}$ space group is a direct compatible subgroup of $R\bar{3}$. The new cell corresponds to: $a_{tricl} = b_{rhombo}$, $b_{tricl} = -a_{rhombo}$, $c_{tricl} = -1/3\,a_{rhombo} + 1/3\,b_{rhombo} + 1/3\,c_{rhombo}$ (refined cell parameters: $a = 4.8457(4)$ Å, $b =$ 4.8464(4) Å, $c = 8.217(1)$ Å, $\alpha = 106.501(6)°$, $\beta =$ 107.497(4)°, and $\gamma = 60.556(4)°$ at 80 K). The cell volume versus temperature (Figure 4b) is concave upward, demonstrating a primary lattice dilatation on cooling.
- Below 75 K, the $R\bar{3}$ symmetry suddenly reappears, while magnetic contributions start growing. The FM ordering is shown by the increasing intensities of the $hk0$ and hkl peaks, while $00l$ remain unchanged. It indicates spins ferromagnetically aligned along c, which is consistent with single-crystal $M(T)$ curves. At 1.8 K, we refined $M(Fe^{2+}) =$ 5.01(7) μ_B ($R_{magn} = 5.38\,\%$). This value confirms a strong orbital contribution already noted from the Curie–Weiss law. As discussed below, this re-entrant phenomenon reflects the competition between the uniaxial magnetism and JT instability.

As shown for Ca_3CoMO_6 (M = Co, Mn, Rh, Ir) and $Fe[C(SiMe_3)_3]_2$,[9] uniaxial magnetism arises when the d states of a d^6 or d^7 HS magnetic ion has unevenly occupied degenerate level (for example, three electrons in a doubly degenerate level) but is also susceptible to JT instability. Uniaxial magnetism can occur only when the level degeneracy is forced by geometry. The 2D FM Ising behavior of $BaFe_2(PO_4)_2$ implies that the HS $Fe^{2+}O_6$ octahedra have uniaxial magnetism along the three-fold rotational axis. Given this, the d states of the FeO_6 octahedron are split into 1a, 1e, and 2e, where the 1a/1e and 2e levels arise from the t_{2g} and e_g manifolds, respectively. Extended Hückel Tight Binding calculations[26] for an isolated FeO_6 octahedron (from 300 K crystal data) show accidentally degenerate 1a and 1e levels (Figure 4c,d). It is consistent with the projected density of states (PDOS) for the Fe 3d states calculated for the FM state of $BaFe_2(PO_4)_2$ (Supporting Information, S3). Therefore, the HS state of the Fe^{2+} ion is described by two electron configurations, $\Phi_1 = (1a)^2(1e)^2(2e)^2$ and $\Phi_2 = (1a)^1(1e)^3(2e)^2$. The Φ_2 configuration with unevenly occupied degenerate level is a necessary requirement for uniaxial magnetism and Ising spins but also favors JT instability. Taking the z axis along the three-fold rotational axis, it is found that, for Fe 3d orbitals, Φ_2 has 69 % ($L = 2$, $S = 2$) character and 31 % ($L = 1$, $S = 2$) character. Under spin–orbit coupling, the first and second components lead to $\Delta J_z = 8$ and 6, respectively, in the lowest-lying doublet state. Then, Φ_2 induces uniaxial magnetism,[9] as $\Delta J_z > 1$. The triclinic distortion below 140 K can be related to the occurrence of a weak JT distortion of each FeO_6 octahedron. The extent of this distortion cannot be strong, as it occurs within the constraint of the 2D layer. The re-entrant structural transition below T_c suggests that the associated lattice contraction cannot support even weak JT distortions, thereby restoring uniaxial magnetism.

We evaluated the three spin exchange parameters J_{1-3} within the honeycomb layer by energy-mapping analysis based on GGA + U calculations[27] (for details, see the Supporting Information, S4).[28] Results (Table 2) show qualitatively similar results for $U = 4$ to 6 eV, which has proven to be reasonable for comparable Fe^{2+} based systems.[29] FM J_1 is predominant, while both J_2 and J_3 are weak. The exact solution of the 2D Ising ferromagnet over a honeycomb lattice with $S = 1$ ions gives the second-order magnetic transition at $T_c = 1.5186\,J k_B^{-1}$.[30] For $S = 2$ ions, J has to be

 © 2012 Wiley-VCH Verlag GmbH & Co. KGaA, Weinheim

Table 2: Magnetic exchange interactions *J* obtained by GGA + U calculations.

		J_1 path (SE)	J_2 path (SSE)	J_3 path (SSE)
J [K]	*U* = 4 eV	28.31	−0.52	1.61
	U = 5 eV	25.22	3.16	4.93
	U = 6 eV	16.84	1.43	3.76

renormalized by $S(S+1)$, leading to $T_c = 4.55\,J\,k_B^{-1}$. Taking $J = J_1 = 16.8$ K from our calculations with $U = 6$ eV and neglecting next-nearest neighbor J_2 and J_3, T_c is calculated to be 76.4 K, in good agreement with its 65.5 K experimental value. Owing to the large interlayer separation, it is not straightforward to determine the corresponding Fe–Fe exchange constant. It was estimated to be negligible owing to the small energy difference ($\Delta E = 0.015$ meV/FU) between the FM and AFM arrangements of FM layers from GGA + U calculations. The coupling between successive FM layers can occur through magnetic dipole–dipole (MDD) interactions, as evidenced in several layered magnetic systems.[21,29] Our calculations of the MDD interaction energies (Supporting Information, S5) indicate that using FM layers with spins aligned parallel to the *c* axis, the FM arrangement between layers is very slightly lower in energy than the AFM state (0.14 meV/FU), but the predominant 2D character is preserved.

Using hydrothermal synthesis with hydrazine as reducing agent in the feeding solution, we successfully prepared $BaFe_2(PO_4)_2$, which consists of honeycomb layers made up of edge-sharing FeO_6 octahedra containing HS Fe^{2+} ions. We showed that $BaFe_2(PO_4)_2$ is a unique oxide with 2D Ising ferromagnetism and undergoes a re-entrant structural transition, which is most probably due to the competition between Jahn–Teller instability and uniaxial magnetism of the FeO_6 octahedra. Work is in progress concerning the possibility of modifying this phase by chemical doping to support spin-polarized transport across the FM layers.

Experimental Section

$Ba(CO_3)_2$/$Fe(Cl)_2{\cdot}4H_2O$ (1.38 g/1.39 g) and H_3PO_4 (2 mL, 65 %) were introduced in a 25 mL Teflon-lined autoclave with hydrazine as reducing agent (1.6 mL). The autoclave was filled up to 20 mL with water, heated up to 220 °C (40 °C h^{-1}) for 72 h, and cooled down to room temperature (4 °C h^{-1}). After washing with water and filtering, single crystals of $BaFe_2(PO_4)_2$ ($100 \times 100 \times 10$ μm^3) were extracted. For powder samples, a microwave-assisted procedure was used to produce $BaFe_2(PO_4)_2$ in high yield in an adapted Teflon-lined vessel. The vessel was then heated at 200 °C (power of 300 W) for 30 min. The non-magnetic $BaHPO_4$ impurity can be removed using successive washing with ethanol.

Diffraction data were collected using a X8-Bruker SMART apex diffractometer ($\lambda = Mo_{K\alpha}$). Intensities were extracted and corrected using the SAINT program.[31] Multi-scan absorption corrections were applied using the SADABS program.[32] The crystal structure refinement was performed using the JANA 2000 program.[33] Further details on the crystal structure investigations may be obtained from the Fachinformationszentrum Karlsruhe, 76344 Eggenstein-Leopoldshafen, Germany (fax: (+49) 7247-808-666; e-mail: crysdata@fiz-karlsruhe.de), on quoting the depository number CSD-424895.

Magnetic measurement data were measured on a MPMS Squid (Quantum Design). Typical measurements were performed using the zero field cooling (ZFC) and field cooling (FC) procedures under a 0.01 T field. Extraction of the critical exponents is described in the Supporting Information, S2.

Received: July 24, 2012
Revised: August 31, 2012
Published online: October 19, 2012

Keywords: 2D ferromagnetism · barium · iron · Jahn–Teller effects · Re-entrant transitions

[1] O. Toulemonde, P. Roussel, O. Isnard, G. André, O. Mentré, *Chem. Mater.* **2010**, *22*, 3807 – 3816.
[2] M. H. Qin, K. F. Wang, J. M. Liu, *Phys. Rev. B* **2009**, *79*, 172405.
[3] M. Lenertz, J. Alaria, D. Stoeffler, S. Colis, A. Dinia, *J. Phys. Chem. C* **2011**, *115*, 17190 – 17196.
[4] H. Kageyama, K. Yoshimura, K. Kosuge, M. Azuma, M. Takano, H. Mitamura, T. Goto, *J. Phys. Soc. Jpn.* **1997**, *66*, 3996 – 4000.
[5] W. Bao, Z. Q. Mao, Z. Qu, J. W. Lynn, *Phys. Rev. Lett.* **2008**, *100*, 247203.
[6] G. Cao, O. Korneta, S. Chikara, L. E. DeLong, P. Schlottmann, *J. Appl. Phys.* **2010**, *107*, 09D718.
[7] Y. Yoshiyuki, I. Shin-Ichi, M. Hirofumi, S. Naoki, C. H. Lee, K. Susumu, *Phys. Rev. B* **2005**, *72*, 054412.
[8] a) G. Ouvrard, E. Sandre, R. Brec, *J. Solid State Chem.* **1988**, *73*, 27 – 32; b) R. E. Marsh, *J. Solid State Chem.* **1988**, *77*, 190 – 191; c) V. Carteaux, F. Moussa, M. Spiesser, *Europhys. Lett.* **1995**, *29*, 251 – 256.
[9] a) D. Dai, M.-H. Whangbo, *Inorg. Chem.* **2005**, *44*, 4407 – 4414; b) Y. Zhang, H. J. Xiang, M.-H. Whangbo, *Phys. Rev. B* **2009**, *79*, 054432; c) Y. Zhang, E. J. Kan, H. J. Xiang, A. Villesuzanne, M.-H. Whangbo, *Inorg. Chem.* **2011**, *50*, 1758.
[10] J. B. Goodenough, *Magnetism And The Chemical Bond*, Wiley-Intersciences, New York, **1963**.
[11] H. Miyamoto, *Mater. Res. Bull.* **1976**, *11*, 329 – 335.
[12] A. Vasiliev, O. Volkova, I. Presniakov, A. Baranov, G. Demazeau, J.-M. Broto, M. Millot, N. Leps, R. Klingeler, B. Büchner, M. B. Stone, A. Zheludev, *J. Phys. Condensed Matter* **2010**, *22*, 016007.
[13] W. Schiessl, W. Potzel, H. Karzel, M. Steiner, G. M. Kalvius, *Phys. Rev. B* **1996**, *53*, 9143 – 9152.
[14] a) Z. Bircsak, W. T. A. Harrison, *Acta Crystallogr. Sect. C* **1998**, *54*, 1554 – 1556; b) J. Dojčilović, M. Napijalo, L. Novaković, M. Napijalo, *Mater. Chem. Phys.* **1990**, *26*, 339 – 345.
[15] a) L. Regnault, P. Burlet, J. Rossat Mignod, *Physica B + C* **1977**, *86*, 660 – 662; b) L. P. Regnault, J. Rossat-Mignod in *Magnetic Properties of Layered Transition Metal Compounds* (Ed.: L. J. De Jongh), Kluwer, Dordrecht, **1990**, pp. 271 – 321 (Ref. [1]).
[16] a) N. Rogado, Q. Huang, J. Lynn, A. Ramirez, D. Huse, R. Cava, *Phys. Rev. B* **2002**, *65*, 144443; b) M. Heinrich, H. Von Nidda, A. Loidl, N. Rogado, R. Cava, *Phys. Rev. Lett.* **2003**, *91*, 137601.
[17] H. Kabbour, E. Janod, B. Corraze, M. Danot, C. Lee, M.-H. Whangbo, L. Cario, *J. Am. Chem. Soc.* **2008**, *130*, 8261 – 8270.
[18] L. P. Regnault, *Contribution à l'étude des excitations non linéaires dans des systèmes uni et bidmensionnels à anisotropie planaire*, PhD thesis, Institut National Polytechnique de Grenoble, **1981**.
[19] Magnétisme: Fondements, E. Du Trémolet de Lacheisserie, EDP Sciences **2000**, p. 199.
[20] S. E. McLain, M. R. Dolgos, D. A. Tennant, J. F. C. Turner, T. Barnes, T. Proffen, B. C. Sales, R. I. Bewley, *Nat. Mater.* **2006**, *5*, 561 – 566.
[21] I. Tong, R. K. Kremer, J. Köhler, A. Simon, C. Lee, E. Kan, M.-H. Whangbo, *Z. Kristallogr.* **2010**, *225*, 498 – 512.
[22] N. D. Mermin, H. Wagner, *Phys. Rev. Lett.* **1966**, *17*, 1133 – 1136.

© 2012 Wiley-VCH Verlag GmbH & Co. KGaA, Weinheim

[23] H. P. Kunkel, R. M. Roshko, G. Williams, *Phys. Rev. B* **1988**, *37*, 5880.
[24] H. E. Stanley, *Introduction to Phase Transitions and Critical Phenomena*, Clarendon, Oxford, **1971**.
[25] L. Wei, H. P. Kunkel, X. Z. Zhou, G. Williams, Y. Mukovskii, D. Shulyatev, *Phys. Rev. B* **2007**, *75*, 012406.
[26] Our calculations were carried out by employing the SAMOA (Structure and Molecular Orbital Analyzer) program package. This program can be downloaded free of charge from the website http://www.primec.com/.
[27] M.-H. Whangbo, H.-J. Koo, D. Dai, *J. Solid State Chem.* **2003**, *176*, 417.
[28] S. L. Dudarev, G. A. Botton, S. Y. Savrasov, C. J. Humphreys, A. P. Sutton, *Phys. Rev. B* **1998**, *57*, 1505.
[29] H.-J. Koo, H. Xiang, C. Lee, M.-H. Whangbo, *Inorg. Chem.* **2009**, *48*, 9051 – 9053.
[30] P. C. Da Silva, U. L. Fulco, F. D. Nobre, L. R. Da Silva, L. S. Lucena, *Braz. J. Phys.* **2002**, *32*, 617 – 623.
[31] *SAINT: Area-Detector Integration Software*, Siemens Industrial. Automation, Inc.: Madison, WI, **1995**.
[32] *SADABS: Area-Detector Absorption Correction*; Siemens Industrial. Automation, Inc.: Madison, WI, **1996**.
[33] V. Petricek, M. Dusek, L. Palatinus, *JANA2006*, Institute of Physics, Academy of Sciences, Praha, Czech Republic, **2006**.

 © 2012 Wiley-VCH Verlag GmbH & Co. KGaA, Weinheim